Forecasting Research

Met O 11 Scientific Note No. 1

The Theory of Periodic Solutions of the Semi-geostrophic Equations

by

R.J. Purser

October 1987

Meteorological Office (Met O 11)
London Road, Bracknell, Berkshire RG12 2SZ, England

MET O 11 SCIENTIFIC NOTE NO. 1

THE THEORY OF PERIODIC SOLUTIONS OF THE SEMIGEOSTROPHIC EQUATIONS

by

R J PURSER

Met O 11 (Forecasting Research)
Meteorological Office
London Road
Bracknell
Berkshire RG12 2SZ
ENGLAND

October 1987

ABSTRACT

The f-plane semi-geostrophic equations have a class of solutions which are periodic in two independent horizontal directions. The large scale flows of such solutions comprise a quadratic geopotential and a wind field whose deformation, vorticity and divergence are, at each instant, spatially uniform, although they may evolve in time. The general conditions that must pertain for these large scale flows confined between parallel horizontal boundaries are established and the equations for the periodic perturbations are derived in co-ordinate frameworks particularly suited to numerical representation.

1. INTRODUCTION

The two-dimensional semi-geostrophic equations (SGE) of Hoskins and Bretherton (1972) were introduced to provide a simplified framework in which to study the essential mechanisms leading to the formation of lower and upper tropospheric fronts. The insights provided by such models have been of immense value in elucidating the significance of purely dynamical processes, and especially those associated with ageostrophic advection, in generating a sharp front from initially smooth conditions. Since that time the SGE have been found to have a natural three-dimensional generalisation (Hoskins, 1975; Hoskins and Draghici, 1977) that in principle allows frontal formation to be studied in more general ambient conditions. A special variant of this set of three-dimensional equations were employed by Hoskins and West (1979) to simulate the formation of fronts associated with a developing baroclinic wave.

The use of the SGE in their Lagrangian conserving form have been shown by Cullen (1983), Cullen and Purser (1984) to allow internally consistent frontal solutions to be integrated beyond the time at which the frontal singularity first forms, thereby permitting a formal extension of the kind of solutions pioneered by Hoskins and Bretherton to be made but with mature fronts involving actual discontinuities of the state variables now figuring as well defined features of the solution. It is the ability of the SGE to tolerate such apparently singular phenomena and handle them in a way that seems consistent with all but the most detailed physical processes that makes this system of equations so attractive, not only as a tool with which to model frontal dynamics, but also as an idealized framework in which to assess the resiliance and reliability of various conventional modelling techniques confronted by singular solutions, so that the best of these techniques may be selected for use with the complete primitive equations in actual forecasting models.

Some of the behaviour exhibited by a model based on the SGE appears at first sight to be a paradoxical contradiction of the general physical principles on which the equations are based, in particular the evolution a front involves a definite <u>increase</u> in domain-integrated potential vorticity and non-vanishing vertical velocity arbitrarily close to the ground near the point of frontal formation. This allows fluid initially in contact with the ground to be lifted well clear. It can be demonstrated that the SGE permit an isolated impulsive concentration of potential vorticity in the interior of the solution to receive or shed some of it from sources or to sinks elsewhere in the fluid or at boundaries without the intervening medium holding any potential vorticity whatsoever. In spite of these paradoxes, the SGE possess an internal consistency and robustness and their solutions, even when they contain singularities, stand as convincing idealized approximations to the kinds of states to be expected in nature in air controlled predominantly by Coriolis balance. In a natural front, of course, the increase of potential vorticity must be accounted for by dissipative processes such as turbulent mixing and such processes may be on a much finer scale than is typically resolved by forecasting models. In that case it might be argued that a finite element model using the SGE which is able to handle sharp discontinuities explicitly is a more reliable guide to the qualitative evolution of a frontal system than a primitive equation model that resolves the fronts poorly.

Apart for a small number of analytic solutions (eg, Gill, 1981; Purser and Cullen, 1987; Shutts, 1987) the most satisfactory method of modelling mature semi-geostrophic fronts in a way that preserves the mathematical discontinuities has been by way of finite element computations (Cullen, 1983; Cullen and Purser, 1984; Cullen et al., 1987). Although such solutions to date have been two-dimensional, it is possible to create solutions to fully three-dimensional flows in terms of simple convex finite elements, the evolution of whose dynamical variables is determined by the geostrophic wind components at their centroids. The assumption that each finite element retains its identity and that its geostrophic momentum components evolve according to the centroid geostrophic wind is justified, on the f-plane at least, by invoking what will be referred to as the 'homogenization postulate' - that internal ageostrophic motion inside each element acts on a timescale faster than that of the large scale motion and has the effect of preserving the element's uniform distribution of potential temperature, and its components of absolute momentum. It can be demonstrated that the resulting dynamical system is energetically consistent when the kinetic energy is taken as coming from only the geostrophic portion of the horizontal velocity. A piecewise continuous semi-geostrophic solution may then be regarded as the limit of a sequence of progressively detailed finite element solutions. It appears very likely, although it has yet to be proved rigorously, that the limit (in an appropriate sense) of the sequence of forecasts from such approximating finite element states is identical to the forecast from the piecewise continuous problem. Should it become feasible to carry out three-dimensional simulations with finite elements it would be possible to integrate approximations to any consistent initial states, including those that give rise to frontal discontinuities.

A problem with three-dimensional semi-geostrophic solutions in a laterally bounded domain is the presence of Kelvin waves. The long, low frequency Kelvin waves are presumably accurately approximated but at higher frequencies the modes produced by the SGE are clearly spurious but are not easily filtered from the solution. It should be noted that even incompressible barotropic flow is contaminated by Kelvin waves in the SGE although they are of course impossible in an unfiltered model. The problems of contamination of the solutions with unwanted Kelvin waves can be avoided by the imposition of doubly cyclic 'boundary' conditions. A solution constrained to be periodic in two horizontal directions permits the influence on the local solution of a surprisingly wide variety of ambient flows to be readily assessed.

It is the purpose of this note first to analyse the general conditions that must pertain on the large scale in order that the imbedded periodic perturbations can be consistently integrated and, second, to show how by suitable time-dependent linear transformations the continuously distorting domain representing a single replication of the general solution can be mapped into a fixed square or cube in a new coordinate system to facilitate the solution of the SGE either by finite difference or by finite element methods.

2. UNIFORM DEFORMATION SOLUTIONS

For algebraic simplicity we adopt the concise notation of Purser and Cullen (1987) henceforth denoted PC. Thus X and Y denote components of geostrophic momentum,

$$X = x + v_g \quad ,$$
$$Y = y - u_g \quad , \tag{2.1a}$$

and Z is proportional to potential temperature,

$$Z = \frac{g}{\theta_0}\theta \tag{2.1b}$$

where the fluid is Boussinesq, hydrostatic and time is rescaled to make the Coriolis parameter unity. Together these components make up a single (column) vector $\underset{\sim}{X}$ which in the terminology of PC is the 'dual' of the corresponding physical coordinate $\underset{\sim}{x} \equiv (x, y, z)^T$. The duality comes about through the symmetrical relationships linking $\underset{\sim}{x}$ and $\underset{\sim}{X}$ to potentials P and R :

$$\left.\begin{array}{l} \underset{\sim}{X} = \underset{\sim}{\nabla}_x P \quad , \\ \\ \underset{\sim}{x} = \underset{\sim}{\nabla}_X R \quad , \end{array}\right\} \tag{2.2}$$

where

$$P = \phi + \tfrac{1}{2}(x^2 + y^2) \quad , \tag{2.3}$$

$$R = \underset{\sim}{x}^T \cdot \underset{\sim}{X} - P \quad , \tag{2.4}$$

and

$$\nabla_x = \left(\frac{\partial}{\partial x}, \frac{\partial}{\partial y}, \frac{\partial}{\partial z}\right)^T ,$$
$$\nabla_X = \left(\frac{\partial}{\partial X}, \frac{\partial}{\partial Y}, \frac{\partial}{\partial Z}\right)^T . \tag{2.5}$$

The basis for the geometrical theory of the SGE on an f-plane is the recognition that dynamically stable solutions are associated with a potential P that is convex in $\mathbf{x}$. In the special extension of SGE whose solutions correspond to finite elements of constant $\mathbf{X}$ the potential, $s = P(\mathbf{x})$, becomes a convex polyhedral 'surface' in the extended domain (s, $\mathbf{x}$). Here we investigate the special class of solutions periodic (in a sense to be defined below) with respect to two independent horizontal <u>lattice basis vectors</u> $\mathbf{\Delta}^{(1)}$, $\mathbf{\Delta}^{(2)}$, which may be time-dependent. It is convenient to augment these vectors with a third,

$$\mathbf{\Delta}^{(3)} = (0, 0, H) \tag{2.6}$$

where H is the total depth of the domain, and group all three into a single matrix $\underline{\underline{\Delta}}$. We shall say that two points $\mathbf{x}^{(1)}$, $\mathbf{x}^{(2)}$ are 'equivalent' points of the solution if they can be expressed

$$\mathbf{x}^{(i)} = \underline{\underline{\Delta}} \cdot \mathbf{a}^{(i)} \qquad i = 1, 2 \tag{2.7}$$

with

$$a_j^{(2)} - a_j^{(1)} = \left\{ \begin{array}{ll} \text{an integer for} & j = 1, 2 \\ 0 & \text{for } j = 3 \end{array} \right\} \tag{2.8}$$

If this is the case the relationship will be expressed

$$\mathbf{x}^{(1)} \sim \mathbf{x}^{(2)}$$

We seek solutions that are periodic in the sense that vector function $\mathbf{X}$ obeys a relation of the form

$$\underset{\sim}{X}(\underset{\sim}{x}^{(2)}) - \underset{\sim}{X}(\underset{\sim}{x}^{(1)}) = \overline{\underset{\approx}{Q}} \cdot (\underset{\sim}{x}^{(2)} - \underset{\sim}{x}^{(1)}) , \qquad (2.9)$$

Whenever $\underset{\sim}{x}^{(2)} \sim \underset{\sim}{x}^{(1)}$, for some uniform, but possibly time-dependent, matrix $\overline{\underset{\approx}{Q}}$. Thus we may split $\underset{\sim}{X}$ into a <u>strictly</u> periodic part $\underset{\sim}{X}'$ plus a part that represents the large scale linear trend, $\overline{\underset{\sim}{X}}$, with,

$$\overline{\underset{\sim}{X}}(\underset{\sim}{x}) = \overline{\underset{\approx}{Q}} \cdot \underset{\sim}{x} + \underset{\sim}{L} \quad . \qquad (2.10)$$

Denoting the cross product and curl operators respectively by '$\wedge$' and '$\underset{\sim}{\nabla}\wedge$' then, since $\underset{\sim}{X}$ is the gradient of a scalar, P, it follows that

$$\underset{\sim}{\nabla}\wedge\overline{\underset{\sim}{X}} + \underset{\sim}{\nabla}\wedge\underset{\sim}{X}' = \underset{\sim}{0} \quad . \qquad (2.11)$$

By applying Stokes' theorem to any basic replication of the horizontal pattern, e. g., the parallelogram formed by the vectors $\underset{\sim}{\Delta}^{(1)}$, $\underset{\sim}{\Delta}^{(2)}$, we see that the average vertical component of $\underset{\sim}{\nabla}\wedge\underset{\sim}{X}'$ and hence of the uniform vector $\underset{\sim}{\nabla}\wedge\overline{\underset{\sim}{X}}$ vanishes. A z-dependent, but horizontally uniform vector may be added to $\underset{\sim}{X}'$ without destroying its periodicity, so it is always possible to partition the vertical shear between $\underset{\sim}{X}'$ and $\overline{\underset{\sim}{X}}$ in such a way that the horizontal components of $\underset{\sim}{\nabla}\wedge\overline{\underset{\sim}{X}}$ and $\underset{\sim}{\nabla}\wedge\underset{\sim}{X}'$ vanish also. Thus $\overline{\underset{\sim}{X}}$ and $\underset{\sim}{X}'$ may be written individually as gradients:

$$\overline{\underset{\sim}{X}} = \underset{\sim}{\nabla}_x \overline{P} = \overline{\underset{\approx}{Q}} \cdot \underset{\sim}{x} + \underset{\sim}{L} \qquad (2.12a)$$

$$\underset{\sim}{X}' = \underset{\sim}{\nabla}_x P' \qquad (2.12b)$$

Where P' is strictly periodic while the large scale trend $\overline{P}$ is now quadratic:

$$\overline{P} = \tfrac{1}{2}\underset{\sim}{x}^{T} \cdot \overline{\underset{\approx}{Q}} \cdot \underset{\sim}{x} + \underset{\sim}{L}^{T} \cdot \underset{\sim}{x} + \overline{P}_0 \qquad (2.13)$$

and $\underset{\approx}{Q}$ is symmetric.

Although the absolute velocities of finite element solutions are not defined within an element, the movement of the facets, edges, and vertices will display a regular linear trend as we move from one replication to another, allowing us to express this trend in the form

$$\bar{U} = \underset{\approx}{S} \cdot \underset{\sim}{x} + \underset{\sim}{V} z + \underset{\sim}{B} \tag{2.14}$$

where $(\underset{\approx}{S} + \underset{\sim}{V} \underset{\sim}{k}^T)$ is the large scale deformation (possibly time-dependent), the portion $\underset{\approx}{S}$ contains that part of the large scale deformation that accounts for the evolution of the basic lattice vectors,

$$\frac{d}{dt} \underset{\approx}{\Delta} = \underset{\approx}{S} \cdot \underset{\approx}{\Delta} \quad , \tag{2.15}$$

while $\underset{\sim}{V}$ expresses the residual vertical shear of the horizontal wind at the large scale. We assume the domain to be bounded at $z = 0$, $z = H$, by horizontal impermeable planes, implying that the large scale component of the velocity vanishes at the ground and is uniformly equal to dH/dt at $z = H$ Thus.

$$\left.\begin{aligned} & S_{31} = S_{32} = S_{13} = S_{23} = 0 \quad , \\ & S_{33} = \frac{1}{H}\frac{dH}{dt} \quad , \\ & V_3 = 0 \quad . \end{aligned}\right\} \tag{2.16}$$

Also, the large scale motion is three-dimensionally non-divergent, implying

$$T_r(\underset{\approx}{S}) = 0 \; . \tag{2.17}$$

In addition to the definitions (2.2), (2.3) the SGE for the evolution of $\underset{\sim}{X}$ are:

$$\left.\begin{aligned} & \frac{D\underset{\sim}{X}}{Dt} = \underset{\sim}{U}_g \\ & \underset{\sim}{\nabla}_x^T \cdot \underset{\sim}{U} = 0 \end{aligned}\right\} \tag{2.18}$$

where D/Dt is the material derivative and $\underset{\sim}{U}_g$ is the geostrophic wind which can be expanded,

$$\underset{\sim}{U}_g = -\underset{\approx}{\mathcal{E}} \cdot (\underset{\sim}{X} - \underset{\sim}{x}) \tag{2.19}$$

with $\underset{\approx}{\mathcal{E}}$ defined,

$$\mathcal{E}_{ij} = \begin{cases} 1 & i=1, j=2 \\ -1 & i=2, j=1 \\ 0 & \text{otherwise}. \end{cases} \tag{2.20}$$

From these equations we deduce the following important result.

Theorem 1

The large scale fields $\overline{\underset{\sim}{X}}$, $\overline{\underset{\sim}{U}}$, $\overline{P}$ are themselves consistent solutions of the SGE independent of the strictly periodic perturbations.

Proof

Define a new time-derivative, $\overline{D}/Dt$, representing the rate of change following the large scale motion $\overline{U}$, ie, for any arbitrary variable ψ :

$$\frac{\overline{D}\psi}{Dt} \equiv \frac{\partial \psi}{\partial t} + (\underset{\sim}{\nabla}_x \psi)^T \cdot \overline{\underset{\sim}{U}} \equiv \frac{D\psi}{Dt} - (\underset{\sim}{\nabla}_x \psi)^T \cdot \underset{\sim}{U}' \tag{2.21}$$

where $\underset{\sim}{U}'$, when it is defined, is the strictly periodic part of $\underset{\sim}{U}$. Note that

$$\frac{\overline{D}\overline{X}}{Dt} = \frac{\partial \overline{X}}{\partial t} + \overline{\underset{\approx}{Q}} \cdot \overline{\underset{\sim}{U}} = \left[\frac{d\overline{\underset{\approx}{Q}}}{dt} + \overline{\underset{\approx}{Q}} \cdot (\underset{\approx}{S} + \underset{\sim}{V}\underset{\sim}{k}^T)\right] \cdot \underset{\sim}{x} + \left(\frac{dL}{dt} + \overline{\underset{\approx}{Q}} \cdot \underset{\sim}{B}\right), \tag{2.22}$$

which is a linear function of position. Also for any pair of equivalent points, $\underset{\sim}{x}^{(1)} \sim \underset{\sim}{x}^{(2)}$ at which we have values $\overline{\underset{\sim}{X}}^{(1)}$, $\overline{X}^{(2)}$ for $\overline{\underset{\sim}{X}}$ and $\underset{\sim}{X}^{(1)}$, $\underset{\sim}{X}^{(2)}$ for $\underset{\sim}{X}$ etc.,

$$\frac{\bar{D}\bar{\underset{\sim}{X}}^{(2)}}{Dt} - \frac{\bar{D}\bar{\underset{\sim}{X}}^{(1)}}{Dt} = \frac{\bar{D}}{Dt}\underset{\sim}{X}^{(2)} - \frac{\bar{D}}{Dt}\underset{\sim}{X}^{(1)}$$

$$= \frac{D\underset{\sim}{X}^{(2)}}{Dt} - \frac{D\underset{\sim}{X}^{(1)}}{Dt} - \underbrace{\left[\underset{\sim}{\nabla}_x \underset{\sim}{X}^{(2)} - \underset{\sim}{\nabla}_x \underset{\sim}{X}^{(1)}\right]^T}_{=0} \cdot \underset{\sim}{u}'$$

$$= \underset{\sim}{u}_g^{(2)} - \underset{\sim}{u}_g^{(1)}$$

$$= \bar{\underset{\sim}{u}}_g^{(2)} - \bar{\underset{\sim}{u}}_g^{(1)} \quad ; \qquad (2.23)$$

where

$$\bar{u}_g = -\underset{\approx}{\varepsilon} \cdot (\bar{\underset{\sim}{X}} - \underset{\sim}{x}) \qquad (2.24)$$

is the large scale part of the geostrophic wind. Since (2.23) is true for all equivalent points and $\bar{D}\bar{X}/Dt$ is linear in position, then generally:

$$\frac{\bar{D}\bar{\underset{\sim}{X}}}{Dt} = \bar{\underset{\sim}{u}}_g + \underset{\sim}{c}(t) \quad . \qquad (2.25a)$$

But the partitioning between $\bar{\underset{\sim}{X}}$ and $\underset{\sim}{X}'$ can always be done so as to eliminate the uniform forcing $\underset{\sim}{c}(t)$ and hence

$$\frac{\bar{D}\bar{\underset{\sim}{X}}}{Dt} = \bar{\underset{\sim}{u}}_g \qquad (2.25b)$$

as required.

<u>Corollary 2</u>

The Hessian $\bar{\underset{\approx}{Q}}$ of the large-scale potential $\bar{P}$ evolves according to

$$\frac{d\bar{\underset{\approx}{Q}}}{dt} + \bar{\underset{\approx}{Q}} \cdot (\underset{\approx}{S} + \underset{\sim}{V}\underset{\sim}{k}^T) + \underset{\approx}{\varepsilon} \cdot (\underset{\approx}{Q} - \underset{\approx}{I}) = 0 \qquad (2.26)$$

and the linear term $\underset{\sim}{L}$ evolves according to

$$\frac{d\underset{\sim}{L}}{dt} + \overline{\underset{\approx}{Q}} \cdot \underset{\sim}{B} + \underset{\approx}{\mathcal{E}} \cdot \underset{\sim}{L} = 0 \qquad . \tag{2.27}$$

These results follow immediately by noting that

$$\overline{U}_g = - \underset{\approx}{\mathcal{E}} \left(\overline{\underset{\approx}{Q}} - \underset{\approx}{I} \right) \underset{\sim}{x} - \underset{\approx}{\mathcal{E}} \cdot \underset{\sim}{L} \tag{2.28}$$

then equating the constant and linear terms of the equation (2.22) when the substitution (2.28) through (2.25b) is made.

The SGE as given have the property that they remain satisfied under non-Galilean but parallel translations in space, provided the transformations,

$$\left.\begin{aligned} \underset{\sim}{x} &= \underset{\sim}{x}^* + \delta \underset{\sim}{x} \\ \underset{\sim}{u} &= \underset{\sim}{u}^* + \delta \underset{\sim}{u} \\ \underset{\sim}{X} &= \underset{\sim}{X}^* + \delta \underset{\sim}{X} \\ P &= P^* + \delta P \end{aligned}\right\} \tag{2.29}$$

in which $\delta \underset{\sim}{x}$, $\delta \underset{\sim}{u}$, $\delta \underset{\sim}{X}$ are spatially uniform (but varying in time) and δP is linear in space, satisfy the transformation rules,

$$\left.\begin{aligned} \delta \underset{\sim}{u} &= \frac{d}{dt} \delta \underset{\sim}{x} \quad , \\ \frac{d}{dt} \delta \underset{\sim}{X} &= - \underset{\approx}{\mathcal{E}} \cdot \left(\delta \underset{\sim}{X} - \delta \underset{\sim}{x} \right) , \\ \underset{\sim}{\nabla}_x \delta P &= \delta \underset{\sim}{X} \quad . \end{aligned}\right\} \tag{2.30}$$

By choosing such a transformation to keep the large scale motion stagnant at the origin the constant terms $\underset{\sim}{L}$ and $\underset{\sim}{B}$ of (2.12a) and (2.14) can be made to vanish, as can $\overline{P}_c$ of (2.13) which consequently simplifies to

$$\overline{P} = \frac{1}{2} \underset{\sim}{x}^T \cdot \overline{\underset{\approx}{Q}} \cdot \underset{\sim}{x} \tag{2.13a}$$

which we use henceforth.

We now consider the constraints governing the evolution of the large scale solutions, for it is clear that the symmetry,

$$\underset{\approx}{Q} = \underset{\approx}{Q}^{T} \tag{2.31}$$

imposes three constraints while (2.16) and (2.17) imply seven more. Then the nine equations (2.26) must be satisfied leaving just three remaining degrees of freedom among H and the components of $\underset{\sim}{V}$, $\underset{\approx}{S}$ and $\overline{\underset{\approx}{Q}}$ to be set at will to make the full set of equations for these large-scale parameters well posed. A convenient set of 'control variables' is formed from the components of $\underset{\approx}{S}$ constituting the horizontal divergence and pure deformation, for example, let

$$\left.\begin{aligned} C_1 &= S_{11} \\ C_2 &= S_{22} \\ C_3 &= S_{12} + S_{21} \end{aligned}\right\} \tag{2.32}$$

Then the remaining components of the deformation field (apart from the vertical divergence which is given by continuity) are the three components of vorticity:

$$\left.\begin{aligned} \zeta_1 &= -V_2 \\ \zeta_2 &= V_1 \\ \zeta_3 &= S_{21} - S_{12} \end{aligned}\right\} \tag{2.33}$$

which cannot be defined independently of the set of control variables $\underset{\sim}{C}$ and Hessian $\overline{\underset{\approx}{Q}}$. Equating the time derivatives of the off-diagonal elements of $\overline{\underset{\approx}{Q}}$ and $\overline{\underset{\approx}{Q}}^{T}$ from (2.26) we find that components $\underset{\sim}{\zeta}$ must satisfy the matrix equation,

$$\begin{bmatrix} \bar{Q}_{12}, & -\bar{Q}_{11}, & \frac{1}{2}\bar{Q}_{23} \\ \bar{Q}_{22}, & -\bar{Q}_{12}, & -\frac{1}{2}\bar{Q}_{13} \\ 0, & 0, & \frac{1}{2}(\bar{Q}_{11}+\bar{Q}_{22}) \end{bmatrix} \cdot \begin{bmatrix} \zeta_1 \\ \zeta_2 \\ \zeta_3 \end{bmatrix} + \begin{bmatrix} 2\bar{Q}_{13}, & \bar{Q}_{13}, & \frac{1}{2}\bar{Q}_{23} \\ \bar{Q}_{23}, & 2\bar{Q}_{23}, & \frac{1}{2}\bar{Q}_{13} \\ \bar{Q}_{12}, & -\bar{Q}_{12}, & \frac{1}{2}(\bar{Q}_{22}-\bar{Q}_{11}) \end{bmatrix} \begin{bmatrix} C_1 \\ C_2 \\ C_3 \end{bmatrix}$$

$$+ \begin{bmatrix} -\bar{Q}_{23} \\ \bar{Q}_{13} \\ 2-\bar{Q}_{11}-\bar{Q}_{22} \end{bmatrix} = \begin{bmatrix} 0 \\ 0 \\ 0 \end{bmatrix} . \qquad (2.34)$$

Note that ζ_3 , which is the only vorticity component to affect the evolution of the latice basis vectors $\underset{\approx}{\Delta}^{(1)}$, $\underset{\sim}{\Delta}^{(2)}$, only depends on the horizontal components of $\bar{\underset{\approx}{Q}}$.

The special class of large-scale solutions that are steady for all time are obtained by setting $d\underset{\approx}{Q}/dt=0$ in (2.26). Then,

$$Q_{13}\, S_{1j} + Q_{23}\, S_{2j} = 0 \qquad j=1,2 \quad ,$$

$$Q_{13}\, V_1 + Q_{23}\, V_2 = 0 \quad . \qquad (2.35)$$

Two distinct cases may arises:

(i) The ratios

$$S_{11} : S_{21} = S_{12} : S_{22} = V_1 : V_2 \quad ,$$

which implies geostrophic parallel shear flow with the velocities perpendicular to the horizontal thermal gradient. Choosing the x-axis parallel to this flow we find

$$\underset{\approx}{Q} \equiv \begin{bmatrix} 1, & 0, & 0 \\ 0, & Q_{22}, & Q_{23} \\ 0, & Q_{23}, & Q_{33} \end{bmatrix}, \quad \underset{\approx}{S} \equiv \begin{bmatrix} 0, & S_{12}, & 0 \\ 0, & 0, & 0 \\ 0, & 0, & 0 \end{bmatrix}, \quad \underset{\sim}{V} \equiv \begin{bmatrix} V_1 \\ 0 \\ 0 \end{bmatrix} \qquad (2.36)$$

with

$$\left.\begin{aligned} S_{12} &= Q_{22} - 1 \\ S_{13} &= Q_{23} \end{aligned}\right\} \qquad (2.37)$$

Such a large scale basic state could be used to investigate baroclinic instabilities on straight jets. In the alternative case,

(ii) The large scale horizontal thermal gradient, and hence the vertical geostrophic and actual wind shears all vanish. Here the flow can most easily be represented by a two-dimensional stream function,

$$\psi = \frac{1}{2} \underset{\sim}{x}^{T} \cdot \underset{\approx}{J} \cdot \underset{\sim}{x} \quad , \qquad (2.38)$$

whose Hessian $\underset{\approx}{J}$ is defined to have no vertical components and to satisfy,

$$\underset{\approx}{S} = -\underset{\approx}{\mathcal{E}} \cdot \underset{\approx}{J} \ . \qquad (2.39)$$

Making this substitution and restricting attention to the horizontal terms only,

$$\underset{\approx}{Q} \cdot \underset{\approx}{\mathcal{E}} \cdot \underset{\approx}{J} = \underset{\approx}{\mathcal{E}} \cdot (\underset{\approx}{Q} - \underset{\approx}{I}) \ . \qquad (2.40)$$

Choosing horizontal axes to diagonalize $\underset{\approx}{Q}$ we find

$$\left.\begin{aligned} J_{11} &= (Q_{11} - 1)/Q_{22} = K_{11}/(K_{22} + 1) \\ J_{22} &= (Q_{22} - 1)/Q_{11} = K_{22}/(K_{11} + 1) \end{aligned}\right\} \qquad (2.41)$$

where $\underset{\approx}{K}$ is the Hessian of the large scale geopotential $\bar{\phi}$.

Having determined the general conditions satisfied by the large scale component of flow we now turn to the construction of the periodic solutions themselves.

3. PERIODIC SOLUTIONS IMBEDDED IN A UNIFORM DEFORMATION

In constructing numerical solutions it is important to recognise explicitly the periodicity present. In the case of finite difference methods we should like to choose coordinates in which the periodic nature of the solution is represented in a convenient way. This is most easily done by projecting the physical coordinates in a manner that causes a single complete replication of the solution to map onto a standard rectangular domain, for example, a unit square or cube. The linear transformation from coordinates $\underset{\sim}{x}$ to co-ordinates $\underset{\sim}{a}$ defined by (2.7) is about the simplest way of accomplishing this. Note that such a transformation in the case of a convex polyhedral (finite element) solution for $P(\underset{\sim}{x})$ gives a transformed $P(\underset{\sim}{a})$ which remains a convex polyhedral solution but now with unit period in the a_1 and a_2 directions. We shall therefore establish the semigeostrophic governing equations as they appear in $\underset{\sim}{a}$-coordinates before specialising further to consider numerical aspects of finite difference and finite element computations separately. We note that an alternative transformation might be well worth applying, that is the linear transformation of dual horizontal coordinates $\underset{\sim}{X}$ to a new pair $\underset{\sim}{b}$ in which the horizontal period is unity in both b_1 and b_2 directions. In the case of a large scale solution free of baroclinity the third coordinate b_3 may be chosen proportional to potential temperature (and hence Z). The resulting framework is well suited to the study of fronts and inversions which are now resolved relatively well, with a regular finite difference grid in $\underset{\sim}{b}$. However, care should be taken over the regions of the interior of $\underset{\sim}{b}$-space that map to the horizontal boundaries and fronts as the governing equations in differential form become singular here. We shall treat a system in $\underset{\sim}{b}$- coordinates at the end of this section.

a. Governing equations in $\underset{\sim}{a}$-coordinates

The differential operator,

$$\underset{\sim}{\nabla}_a \equiv \left(\frac{\partial}{\partial a_1}, \frac{\partial}{\partial a_2}, \frac{\partial}{\partial a_3} \right)^T \quad , \tag{3.1}$$

is related to $\underset{\sim}{\nabla}_x$ by the chain rule:

$$\underset{\sim}{\nabla}_a = \underset{\approx}{\Delta}^T \cdot \underset{\sim}{\nabla}_x \tag{3.2}$$

Define

$$\underset{\sim}{A} = \underset{\sim}{\nabla}_a P = \underset{\approx}{\Delta}^T \cdot \underset{\sim}{X} \tag{3.3}$$

Then

$$\frac{D\underset{\sim}{A}}{Dt} = \left(\frac{d\underset{\approx}{\Delta}^T}{dt}\right)\underset{\sim}{X} + \Delta^T \frac{D}{Dt}\underset{\sim}{X} \quad ,$$

$$= \underset{\approx}{\Delta}^T \cdot \underset{\approx}{S}^T \cdot \underset{\sim}{X} - \underset{\approx}{\Delta}^T \cdot \underset{\approx}{\varepsilon} \cdot (\underset{\sim}{X} - \underset{\sim}{x}) \, ,$$

$$= \underset{\approx}{\eta} \cdot \underset{\sim}{A} + \underset{\approx}{\varepsilon}_a \cdot \underset{\sim}{a} \quad , \tag{3.4}$$

where we have used (2.18), (2.19) and where $\underset{\approx}{\eta}$ and $\underset{\approx}{\varepsilon}_a$ are the matrices:

$$\left.\begin{aligned} \underset{\approx}{\eta} &= \underset{\approx}{\Delta}^T \cdot (\underset{\approx}{S}^T - \underset{\approx}{\varepsilon})(\underset{\approx}{\Delta}^T)^{-1} \quad , \\ \underset{\approx}{\varepsilon}_a &= \underset{\approx}{\Delta}^T \cdot \underset{\approx}{\varepsilon}\, \underset{\approx}{\Delta} \equiv \mathrm{Det}(\underset{\approx}{\Delta}_h)\, \underset{\approx}{\varepsilon} \end{aligned}\right\} \tag{3.5}$$

and where $\underset{\approx}{\Delta}_h$ is the horizontal portion of $\underset{\approx}{\Delta}$.

The continuity equation in $\underset{\sim}{a}$-coordinates retains the same form,

$$\underset{\sim}{\nabla}_a^T \cdot \underset{\sim}{U}_a = 0 \quad , \tag{3.6}$$

where

$$\underset{\sim}{U}_a = \frac{D}{Dt}\underset{\sim}{a} \quad . \tag{3.7}$$

We shall consider convenient representation of these equations for finite difference and finite element computations separately.

(i) Finite difference computations

Here it is convenient to split the variables into their large scale contributions and the strictly periodic portions:

$$\underset{\sim}{A} = \bar{\underset{\sim}{A}} + \underset{\sim}{A}' \equiv \underset{\sim}{\nabla}_a \bar{P} + \underset{\sim}{\nabla}_a P' ,$$

$$\underset{\sim}{\nabla}_a \underset{\sim}{A}^T = \underset{\approx}{Q}_a \equiv \bar{\underset{\approx}{Q}}_a + \underset{\approx}{Q}_a' , \tag{3.8}$$

where

$$\bar{\underset{\sim}{A}} = \bar{\underset{\approx}{Q}}_a \cdot \underset{\sim}{a} .$$

Note that the advantage of $\underset{\sim}{a}$-coordinates is that the large-scale part of $\underset{\sim}{U}_a$ disappears. Hence, from (3.4),

$$\frac{D\underset{\sim}{A}}{Dt} \equiv \frac{\partial \bar{\underset{\sim}{A}}}{\partial t} + \underset{\approx}{Q}_a \cdot \underset{\sim}{U}_a + \frac{\partial \underset{\sim}{A}'}{\partial t} = \underset{\approx}{\eta} \cdot \bar{\underset{\sim}{A}} + \underset{\approx}{\eta} \cdot \underset{\sim}{A}' + \underset{\sim}{\mathcal{E}}_a \cdot \underset{\sim}{a} \tag{3.9}$$

By straight forward evaluation, using (2.26) it can be verified that

$$\frac{\partial \bar{\underset{\sim}{A}}}{\partial t} = \underset{\approx}{\eta} \cdot \bar{\underset{\sim}{A}} + \underset{\approx}{\mathcal{E}}_a \cdot \underset{\sim}{a} \tag{3.10}$$

so the periodic perturbations satisfy

$$\frac{\partial \underset{\sim}{A}'}{\partial t} = \underset{\approx}{\eta} A' - \underset{\approx}{Q}_a \cdot \underset{\sim}{U}_a , \tag{3.11}$$

or, in terms of the perturbation mass field P', and its tendency, $\Gamma' = \left.\frac{\partial P'}{\partial t}\right|_{\underset{\sim}{a}}$,

$$\underset{\approx}{Q}_a^{-1} \cdot \underset{\sim}{\nabla}_a \Gamma' = \underset{\approx}{Q}_a^{-1} \cdot \underset{\approx}{\eta} \cdot \underset{\sim}{\nabla}_a P' - \underset{\sim}{U}_a . \tag{3.12}$$

On eliminating the velocity $\underset{\sim}{U}_a$ using continuity, we arrive at a nonlinear elliptic equation for the tendency:

$$\underset{\sim}{\nabla}_a \cdot \underset{\approx}{Q}_a^{-1} \cdot \underset{\sim}{\nabla}_a \Gamma' = \underset{\sim}{\nabla}_a \cdot \underset{\approx}{Q}_a^{-1} \cdot \underset{\approx}{\eta} \cdot \underset{\sim}{\nabla}_a P' , \tag{3.13}$$

which may be solved by standard iterative methods subject to the boundary conditions implied by the vanishing of $\underset{\sim}{a}$ - space vertical velocity, bottom and top:

$$U_{a(3)} = 0 \quad , \quad a_3 = \begin{cases} 0 \\ 1 \end{cases} \tag{3.14}$$

and horizontal periodicity

$$\Gamma'(\underset{\sim}{a}_2) = \Gamma'(\underset{\sim}{a}_1) \quad , \quad \underset{\sim}{a}_1 \sim \underset{\sim}{a}_2 \quad . \tag{3.15}$$

Eq (3.13) is no harder to solve in principle than the standard semigeostrophic tendency equations (e.g., Schubert, 1985) and transformations back to physical space are easily accomplished. Note that a class of periodic two-dimensional solutions can be obtained by assuming that the strictly periodic variables are invariant with respect to a_2-coordinate (but this does not imply that $U_{a(2)}$-**vanishes**). The tendency equation (3.13) then reduces to a two-dimensional elliptic system in (a1, a3). The two-dimensional systems that can be obtained in this way are apparently generalizations of those discussed by Hoskins and Bretherton (1972).

ii. Finite element computations

The finite element solutions are constructed from the boundary of the region formed in the extended (S, $\underset{\sim}{a}$) - space by the set-intersection of half planes bounded 'below' by the hyperplanes of the form

$$S = S_0 + \underset{\sim}{A}^T \cdot \underset{\sim}{a} \tag{3.16}$$

such that the mass ($\equiv$ volume) $M_0^{(\alpha)}$ of each element α is correct and the element-averaged equations of motion are satisfied,

$$\frac{d}{dt}\left(M_0^{(\alpha)}\underset{\sim}{A}^{(\alpha)}\right) = \underset{\approx}{\eta}\cdot\left(M_0^{(\alpha)}\underset{\sim}{A}^{(\alpha)} + \underset{\approx}{\mathcal{E}}_a \cdot \underset{\sim}{M}_a^{(\alpha)}\right. , \tag{3.17}$$

where $\underset{\sim}{M}_a^{(\alpha)}$ represents the vector of first moments about the origin of element α. Rather than use these moments it will be convenient to choose a set that are identical for different replications of the same element. A natural choice is the set

$$\hat{\underset{\sim}{M}}_a^{(\alpha)} = \underset{\sim}{M}_a^{(\alpha)} - M_0 \underset{\sim}{b}^{(\alpha)} \qquad (3.18)$$

where

$$\underset{\sim}{b}^{(\alpha)} = \underset{\approx}{\bar{Q}}_a^{-1} \cdot \underset{\sim}{A}^{(\alpha)} . \qquad (3.19)$$

Geometrically, $\underset{\sim}{b}^{(\alpha)}$ is the $\underset{\sim}{a}$-coordinate of the point on a quadratic surface,

$$s = \hat{s}_0^{(\alpha)} + \frac{1}{2} \underset{\sim}{a}^T \cdot \underset{\approx}{\bar{Q}}_a \cdot \underset{\sim}{a} , \qquad (3.20)$$

which is tangent to the element's hyperplane

$$s = s_0^{(\alpha)} + \underset{\sim}{A}^{(\alpha)T} \cdot \underset{\sim}{a} . \qquad (3.21)$$

The schematic illustration of Figure 1 should clarify the situation.

Note that $\hat{s}_0^{(\alpha)}$ is common to all equivalent replications of the element α and is related to $s_0^{(\alpha)}$ through

$$\hat{s}_0^{(\alpha)} = s_0^{(\alpha)} + \frac{1}{2} \underset{\sim}{b}^{(\alpha)T} \cdot \underset{\approx}{\bar{Q}}_a \cdot \underset{\sim}{b}^{(\alpha)} . \qquad (3.22)$$

The sensitivity of moments $\underset{\sim}{M}^{(\alpha)} \equiv (M_0^{(\alpha)}, \underset{\sim}{M}_a^{(\alpha)})$ to variations in $\underset{\sim}{S}^{(\beta)} \equiv (s_0^{(\beta)}, \underset{\sim}{A}^{(\beta)})$ is expressed by the symmetric Jacobian matrix of coefficients:

$$\frac{\partial \underset{\sim}{M}^{(\alpha)}}{\partial \underset{\sim}{s}^{(\beta)}} \equiv \frac{-1}{|A^{(\alpha)} - A^{(\beta)}|} \left[\begin{array}{c|c} m_{(\alpha,\beta)} & \underset{\sim}{m}^{T}_{a(\alpha,\beta)} \\ \hline \underset{\sim}{m}_{a(\alpha,\beta)} & \underset{\approx}{m}_{aa(\alpha,\beta)} \end{array} \right], \quad \alpha \neq \beta . \tag{3.23}$$

with $$\frac{\partial \underset{\sim}{M}^{(\alpha)}}{\partial \underset{\sim}{s}^{(\alpha)}} = -\sum_{\beta \neq \alpha} \frac{\partial \underset{\sim}{M}^{(\alpha)}}{\partial s^{(\beta)}} , \tag{3.24}$$

where the summation in (3.24) extends over all elements, including replications, and the components in the block-matrix of (3.23) are defined as follows:

$m_{(\alpha,\beta)}$ is the <u>area</u> (scalar) of the interface between α and β

$\underset{\sim}{m}_{a(\alpha,\beta)}$ is the <u>first moment</u> (vector) " " " " " " "

$\underset{\approx}{m}_{aa(\alpha,\beta)}$ is the <u>second moment</u> (tensor) " " " " " " " .

A corresponding Jacobian expressing the sensitivity of moments $\underset{\sim}{\hat{M}}^{(\alpha)}$ to variations in $\underset{\approx}{\hat{s}}^{(\beta)} \equiv (\hat{s}_o^{(\beta)}, \underset{\sim}{A}^{(\beta)})^T$ is obtained by noting from (3.18) and (3.22) that

$$\left. \begin{aligned} \underset{\sim}{\hat{M}}^{(\alpha)} &\equiv \underset{\approx}{B}^{(\alpha)} \cdot \underset{\sim}{M}^{(\alpha)} \\ \frac{\partial}{\partial \hat{s}^{(\alpha)}} &\equiv \underset{\approx}{B}^{(\alpha)} \cdot \frac{\partial}{\partial s^{(\alpha)}} \end{aligned} \right\} \tag{3.25}$$

where

$$\underset{\approx}{B}^{(\alpha)} = \left[\begin{array}{c|c} 1 & 0 \\ \hline -\underset{\sim}{b}^{(\alpha)} & \underset{\approx}{I} \end{array} \right] , \tag{3.26}$$

and hence by application of the chain rule:

$$\frac{\partial \hat{M}^{(\alpha)}}{\partial \hat{s}^{(\beta)}} = B^{(\alpha)} \cdot \frac{\partial \underset{\sim}{M}^{(\alpha)}}{\partial s^{(\beta)}} \cdot B^{(\beta)T} - M_o^{(\alpha)} \delta_{\alpha\beta} \left[\begin{array}{c:c} 0 & 0 \\ \hdashline 0 & \overline{\underset{\approx}{Q}}_a^{-1} \end{array} \right] . \tag{3.27}$$

Now, not only is $\frac{\partial \hat{M}^{(\alpha)}}{\partial \hat{s}^{(\beta)}}$ symmetric, but moreover it is invariant with respect to simultaneous and corresponding transformations of the pair α, β to any equivalent replication α', β'. Thus the symmetric matrix,

$$\mathbb{J}_{\alpha\beta} = \sum_{\beta' \sim \beta} \frac{\partial \hat{M}^{(\alpha)}}{\partial \hat{s}^{(\beta')}} , \tag{3.28}$$

expresses the sensitivity of each moment $\hat{M}_i^{(\alpha)}$ to simultaneous equivalent change of all equivalent replications of a variable $\hat{s}_j^{(\beta)}$ and the indices α, β need only extend over one non-redundant representation of the set of finite elements (i.e., without replications) in order to encapsulate the information needed to construct a geometric solution (e.g., by Newton iterations) consistent with prescribed gradients $\underset{\sim}{A}^{(\alpha)}$ and masses $M_o^{(\alpha)}$.

The information from the Jacobian matrix $\mathbb{J}_{\alpha\beta}$ may also be applied in solving the element averaged equations of motion implicitly, but in this case we rewrite (3.17) in terms of the modified moments $\hat{M}$:

$$\frac{d}{dt}\left(\hat{M}_o^{(\alpha)} \underset{\sim}{A}^{(\alpha)}\right) = \underset{\approx}{\hat{\eta}} \cdot \left(\hat{M}_o^{(\alpha)} \underset{\sim}{A}^{(\alpha)}\right) + \underset{\approx}{\varepsilon}_a \cdot \underset{\sim}{\hat{M}}_a^{(\alpha)} , \tag{3.17a}$$

where

$$\hat{\eta} = \underset{\sim}{\eta} - \underset{\approx}{\varepsilon}_a \cdot \overline{\underset{\approx}{Q}}_a^{-1} . \tag{3.29}$$

The simplest and most symmetric way to solve (3.17a) implicitly is, first, to construct a vector of residuals $\underset{\sim}{\mathbb{R}} \equiv \left\{ \mathbb{R}^{(\alpha)} \right\}$ where $\mathbb{R}^{(\alpha)} = \left(\mathbb{R}_o^{(\alpha)}, \mathbb{R}_a^{(\alpha)} \right)^T$

and, for timestep δt ,

$$\mathbb{R}_{o\ t+\delta t}^{(\alpha)} = M_{o\ t+\delta t}^{(\alpha)} - M_{o}^{(\alpha)}$$

$$\underset{\sim}{\mathbb{R}}_{a\ t+\delta t}^{(\alpha)} = \left(\frac{\underset{\approx}{I}}{\delta t} - \frac{1}{2}\hat{\underset{\approx}{\eta}}\right)_{t+\delta t} M_{o\ t+\delta t}^{(\alpha)} \underset{\sim}{A}_{t+\delta t}^{(\alpha)} - \frac{\underset{\approx}{\mathcal{E}}_{a\ t+\delta t}}{2} \cdot \hat{\underset{\sim}{M}}_{a\ t+\delta t}^{(\alpha)}$$

$$- \left(\frac{\underset{\approx}{I}}{\delta t} + \frac{1}{2}\hat{\underset{\approx}{\eta}}\right)_{t} M_{o\ t}^{(\alpha)} \underset{\sim}{A}_{t}^{(\alpha)} - \frac{\underset{\approx}{\mathcal{E}}_{a\ t}}{2} \hat{\underset{\sim}{M}}_{a\ t}^{(\alpha)} \quad . \qquad (3.30)$$

The residuals $\underset{\sim}{\mathbb{R}}$ are sensitive to infinitesimal variations of the vectors $\hat{\underset{\sim}{M}}$, $\hat{s}$ in a way that may be expressed symbolically:

$$\delta \underset{\sim}{\mathbb{R}}_{t+\delta t}^{(\alpha)} = \underset{\approx}{\mathbb{K}}_{t+\delta t} \cdot \delta \hat{\underset{\sim}{s}}_{t+\delta t}^{(\alpha)} + \underset{\approx}{\mathbb{L}}_{t+\delta t}^{(\alpha)} \cdot \delta \hat{\underset{\sim}{M}}_{t+\delta t}^{(\alpha)}$$

$$- \underset{\approx}{\mathbb{M}}_{t}^{(\alpha)} \cdot \delta \hat{s}_{t}^{(\alpha)} - \underset{\approx}{\mathbb{N}}_{t}^{(\alpha)} \cdot \delta \hat{\underset{\sim}{M}}_{t}^{(\alpha)} \quad . \qquad (3.31)$$

The (sparse) coefficients of the matrices $\mathbb{K}$, $\mathbb{L}$, $\mathbb{M}$, $\mathbb{N}$ can be immediately obtained from (3.30). Taking into account the sensitivity of $\hat{\underset{\sim}{M}}^{(\alpha)}$ to changes in $\hat{s}^{(\beta)}$ at each time level, treating $\underset{\approx}{\mathbb{K}}$ as a block diagonal matrix of blocks $\underset{\approx}{\mathbb{K}}^{(\alpha)}$, and similarly for $\mathbb{L}$, $\mathbb{M}$, $\mathbb{N}$:

$$\delta \underset{\sim}{\mathbb{R}} = \left(\underset{\approx}{\mathbb{K}}_{t+\delta t} + \underset{\approx}{\mathbb{J}}_{t+\delta t} \cdot \underset{\approx}{\mathbb{L}}_{t+\delta t}\right) \cdot \delta \hat{\underset{\sim}{s}}_{t+\delta t} - \left(\underset{\approx}{\mathbb{M}}_{t} + \underset{\approx}{\mathbb{J}}_{t} \cdot \underset{\approx}{\mathbb{N}}_{t}\right) \cdot \delta \hat{\underset{\sim}{s}}_{t} \quad . \qquad (3.32)$$

Thus in the conventional forward integration the vector of residuals $\underset{\sim}{\mathbb{R}}$ can be made to vanish by a Newton iteration involving the matrix ($\mathbb{K}_{t+\delta t} + \mathbb{J}_{t+\delta t} \cdot \mathbb{L}_{t+\delta t}$)

The equation (3.32) also informs us of the sensitivity of the solution to variations in the values of the previous time level, since, conditional on the vanishing of $\delta \mathbb{R}$, we have symbolically the sensitivity matrix:

$$\frac{\partial \hat{\underset{\sim}{s}}_{t+\delta t}}{\partial \hat{\underset{\sim}{s}}_t} = \left(\underset{\approx}{\mathbb{K}}_{t+\delta t} + \underset{\approx}{\mathbb{J}}_{t+\delta t} \cdot \underset{\sim}{\mathbb{L}}_{t+\delta t}\right)^{-1} \left(\underset{\approx}{\mathbb{M}}_t + \underset{\approx}{\mathbb{J}}_t \cdot \underset{\approx}{\mathbb{N}}_t\right) \quad . \tag{3.33}$$

Thus, having obtained and stored a time dependent solution and the sequence of Jacobian coefficients $\mathbb{J}_t$, it is quite straight-forward to conduct linear sensitivity studies about this solution, for example, the effect of an initial infinitesimal perturbation $\delta \underset{\sim}{\hat{s}}_0$ of $\underset{\sim}{\hat{s}}$ at $t = 0$ implies a change at a later time given by chaining the matrices of (3.33):

$$\delta \underset{\sim}{\hat{s}}_t = \frac{\partial \hat{\underset{\sim}{s}}_t}{\partial \hat{\underset{\sim}{s}}_{t-\delta t}} \cdot \frac{\partial \hat{\underset{\sim}{s}}_{t-\delta t}}{\partial \hat{\underset{\sim}{s}}_{t-2\delta t}} \cdot \cdot \cdot \frac{\partial \hat{\underset{\sim}{s}}_{\delta t}}{\partial \hat{\underset{\sim}{s}}_0} \cdot \delta \hat{\underset{\sim}{s}}_0 \tag{3.34}$$

With evaluations proceeding from right to left in order to avoid matrix-matrix multiplies. Alternatively, using the same matrices (or rather, their transposes), we may investigate the adjoint problem in order to find to which variables $\hat{\underset{\sim}{s}}_0$ is a particular linear function of the variations $\hat{\underset{\sim}{s}}_t$ sensitive:

$$\frac{\partial \lambda}{\partial \hat{\underset{\sim}{s}}_0} \equiv \left(\frac{\partial \hat{\underset{\sim}{s}}_{\delta t}}{\partial \hat{\underset{\sim}{s}}_0}\right)^T \cdot \cdot \cdot \left(\frac{\partial \hat{\underset{\sim}{s}}_{t-\delta t}}{\partial \hat{\underset{\sim}{s}}_{t-2\delta t}}\right)^T \left(\frac{\partial \hat{\underset{\sim}{s}}_t}{\partial \hat{\underset{\sim}{s}}_{t-\delta t}}\right)^T \frac{\partial \lambda}{\partial \hat{\underset{\sim}{s}}_t} \quad . \tag{3.35}$$

When $\left(\underset{\approx}{\mathbb{M}}_t + \underset{\approx}{\mathbb{J}}_t \cdot \underset{\approx}{\mathbb{N}}_t\right)$ are invertible at each t (note that singularities due to the freedom to vary the mean geopotential are trivially removed) we may also integrate the perturbation equations back in time. All such linear operations avoid the need to reconstruct the geometry of the finite elements which for large problems is the dominant part of the computations. However, they do require storage of the basic solution and of the principal Jacobian matrix $\mathbb{J}$ at each time.

By an extension of the differential (3.31) to include variations of $\underset{\approx}{\mathcal{E}}_a$ and $\hat{\underset{\approx}{\eta}}$ consequent upon revisions in the evolution of the large scale component of the solution it is possible to investigate directly the effect that the large scale deformation has on the small scale periodic perturbation, again without the laborious recalculation of the geometry of the finite elements being necessary. it is possible to envisage a further range of linear sensitivity studies that could be carried out with the finite element model if diabatic and viscous effects are incorporated into the system in some way that leaves the elements 'flat' in $(s, \underset{\sim}{a})$-space.

b. Governing equations in $\underset{\sim}{b}$-coordinates

We complete this section with a brief discussion of finite difference methods expressed in coordinates regular in the space of the variable $\underset{\sim}{b}$ defined by (3.19). The motivation for this choice is that fronts and inversions will be better resolved than in $\underset{\sim}{a}$-space while the simple unit periodicity in the two orthogonal horizontal directions is preserved. However, it is probably not feasible to carry out extended integrations in $\underset{\sim}{b}$-coordinates unless the large-scale motion is not baroclinic, otherwise it is difficult to guess beforehand the range of the third coordinate b_3 needed to accommodate the whole evolution of the solution (as large-scale available potential energy is released in the course of an integration the range of potential temperature, and hence of b_3, in the solution at a given location [b_1, b_2] will tend to increase). When the large scale flow is horizontally stratified, then b_3 is proportional to potential temperature and consequently adiabatic motion in $\underset{\sim}{b}$ - space is exactly horizontal. This motion may be expressed as a 'velocity', $\underset{\sim}{u}_b$, defined by

$$\underset{\sim}{u}_b = \frac{D\underset{\sim}{b}}{Dt} \quad . \tag{3.36}$$

Note that

$$\frac{D}{Dt}\left(\overline{\underset{\approx}{Q}}_a \cdot \underset{\sim}{b}\right) = \frac{\partial \overline{\underset{\approx}{Q}}_a}{\partial t} \cdot \underset{\sim}{b} + \overline{\underset{\approx}{Q}}_a \cdot \underset{\sim}{u}_b = \frac{D\underset{\sim}{A}}{Dt} \tag{3.37}$$

From (3.9) and (3.19)

$$\left(\underset{\approx}{\eta} \cdot \overline{\underset{\approx}{Q}}_a + \underset{\approx}{\varepsilon}_a\right) \cdot \underset{\sim}{b} + \overline{\underset{\approx}{Q}}_a \cdot \underset{\sim}{u}_b = \underset{\approx}{\eta} \cdot \overline{\underset{\approx}{Q}}_a \cdot \underset{\sim}{b} + \underset{\approx}{\varepsilon}_a \cdot \underset{\sim}{a} \tag{3.38}$$

i.e.,

$$\overline{\underset{\approx}{Q}}_a \cdot \underset{\sim}{u}_b = \underset{\approx}{\varepsilon}_a \cdot (\underset{\sim}{a} - \underset{\sim}{b}) \quad . \tag{3.39}$$

At this stage we invoke the dual potential of (2.4) which, in terms of $\underset{\sim}{a}$ and $\underset{\sim}{A}$ variables is

$$R = \underset{\sim}{a}^T \cdot \underset{\sim}{A} - P \tag{3.40}$$

with $\underset{\sim}{a}$ given by the gradient in $\underset{\sim}{A}$ - space of R:

$$\underset{\sim}{a} = \underset{\sim}{\nabla}_A R = \overline{\underset{\approx}{Q}}_a^{-1} \cdot \underset{\sim}{\nabla}_b R \tag{3.41}$$

Hence

$$\underset{\sim}{u}_b = \underset{\approx}{\mathcal{E}}_b \cdot \underset{\sim}{\nabla}_b R' \tag{3.42}$$

where

$$\underset{\approx}{\mathcal{E}}_b = \overline{\underset{\approx}{Q}}_a^{-1} \cdot \underset{\approx}{\mathcal{E}}_a \cdot \overline{\underset{\approx}{Q}}_a^{-1} \equiv \left(\frac{\mathrm{Det}\, \overline{\underset{\approx}{Q}}_h}{\mathrm{Det}\, \underset{\approx}{\Delta}_h} \right) \underset{\approx}{\mathcal{E}} \tag{3.43}$$

and the stream function,

$$R' = R - \overline{R}$$

$$\overline{R} = \frac{1}{2} \underset{\sim}{b}^T \cdot \overline{\underset{\approx}{Q}}_a \cdot \underset{\sim}{b} \tag{3.44}$$

implies non-divergent flow in $\underset{\sim}{b}$ - space. Note that R' is the strictly periodic part of R.

The conservation of mass and potential vorticity translates to $\underset{\sim}{b}$-space as the conservation of

$$\rho_b = \mathrm{Det}\, (\underset{\approx}{Q}_b) \tag{3.45}$$

where $\underset{\approx}{Q}_b$ is the Hessian of R :

$$\underset{\approx}{Q}_b = \underset{\sim}{\nabla}_b \underset{\sim}{\nabla}_b^T R \tag{3.46}$$

Note that from the definition of ρ_b ,

$$\delta(\log \rho_b) = Tr\left(Q_b^{-1} \cdot \delta Q_b\right) \quad , \tag{3.47}$$

hence the Lagrangian conservation of log ρ_b expressed in terms of R' gives,

$$\sum_{i,j=1}^{3} Q_{b\,ij}^{-1} \frac{\partial^2 \left(\frac{\partial R'}{\partial t}\right)}{\partial b_i \partial b_j} + Tr\left(Q_b^{-1} \cdot \frac{d\bar{Q}_a}{dt}\right) + \frac{1}{\rho_b} (\nabla_b \rho_b)^T \underset{\approx}{\varepsilon}_b \cdot \nabla_b R' = 0 \tag{3.48}$$

in which the left term is written in suffix notation to emphasize that this is a linear elliptic equation, with varying coefficients, for $\frac{\partial R'}{\partial t}$. Notice that all the terms in this equation are strictly periodic. The top and bottom boundary conditions required to completed the system come from the vanishing of the material derivative of $\underset{\sim}{a}_3$ which, since the large scale flow is assumed non-baroclinic, can be expressed

$$\begin{aligned} \frac{d\bar{Q}_{a_{33}}}{dt} a_3 &= \frac{D}{Dt}\left(\underset{\approx}{\bar{Q}}_a \cdot \underset{\sim}{a}\right)_3 = \frac{D}{Dt}\left(\frac{\partial R}{\partial b_3}\right) \\ &= \frac{d\bar{Q}_{33}}{dt} b_3 + \frac{\partial}{\partial b_3}\left(\frac{\partial R'}{\partial t}\right) + \left(\nabla_b \frac{\partial R'}{\partial b_3}\right)^T \cdot \underset{\approx}{\varepsilon}_b \cdot \underset{\sim}{\nabla}_b R' \end{aligned} \tag{3.49}$$

But if the boundaries where this equation applies are $a_3 = b_3 = 0$ and $a_3 = b_3 = 1$, the condition reduces to

$$\frac{\partial}{\partial b_3}\left(\frac{\partial R'}{\partial t}\right) + \left(\underset{\sim}{\nabla}_b \frac{\partial R'}{\partial b_3}\right)^T \cdot \underset{\approx}{\varepsilon}_b \cdot \underset{\sim}{\nabla}_b R' = 0 \tag{3.50}$$

Note that although many interesting problems would appear to be excluded by the assumption that b_3 , and hence θ , is constant on the top and bottom boundaries (for example, Cullen and Purser (1984) show that frontogenesis can not occur under such conditions) more general <u>effective</u> boundary conditions that allow undulations in the boundary of the region of $\underset{\sim}{b}$ - space containing values of ρ_b of significant magnitude can still be admitted by 'padding' the zone between this effective boundary and the true boundary (e.g., $b_3 = 0$) with values of ρ_b that are very small but positive. In $\underset{\sim}{a}$ -space and hence in physical space this padded region maps to a very shallow layer of extremely high potential vorticity confined to hug the boundary or, in appropriate circumstances, to fill narrow frontal zones. Being of negligible mass it is not expected to alter the physical solution significantly. A schematic illustration of this method is provided in Figure 2.

4. SUMMARY AND DISCUSSION

By assuming semi-geostrophic solutions in the geopotential that, apart from a large scale quadratic variation, are periodic in two horizontal directions it has been shown that this large-scale component itself remains an exact solution of the SGE. The form of the large scale solution is determined at each time by the matrices representing the Hessian of the geopotential and the deformation for the velocity. It is shown that the evolution of these matrices in the general case is constrained in several ways but that three free 'steering' parameters remain and must be prescribed at each time in order to specify a unique and consistent evolution. These parameters may be taken to be the two components of horizontal pure deformation and the horizontal divergence at the large scale; the remaining large-scale wind variations, i.e., the vorticity and the vertical shear are then automatically constrained by the conservation of potential vorticity and of potential temperature for semigeostrophically balanced motion.

Equations are derived for the strictly periodic perturbations both for finite difference and for finite element modelling. A special class of the finite difference equations gives rise to a two-dimensional periodic system generalizing those discussed by Hoskins and Bretherton (1972). It is found that, when the large-scale component of the flow is not baroclinic the system lends itself to numerical treatment in the 'dual' lattice coordinates in which fronts and inversions (usually small-scale in cross-section) automatically become well resolved by a regular grid and consequently these coordinates would be attractive for investigating idealized frontal dynamics.

The periodic formulations conveniently avoid the difficult task of removing the spurious Kelvin edge waves that invariably contaminate semigeostrophic solutions constructed within domains bounded laterally by rigid walls. In the context of improving numerical techniques for forecasting, the semigeostrophic models provide an ideal framework for checking the robustness and accuracy of finite difference methods that in real-life forecasting applications must contend with sharp transitions in velocity or potential temperature. These singular 'frontal' features are mathematically well behaved in semigeostrophic dynamics so the correct solution to any problem can presumably be ascertained in practice by solving it at a sufficient numerical resolution, while the corresponding structures in a primitive equation formulation are liable to be dependent on the particular techniques employed to remove grid-scale energy (it is doubtful whether the inviscid primitive equations constitute a well posed system mathematically).

At a theoretical level, the periodic semigeostrophic models might be used to elucidate the extent to which large-scale deformation, convergence or divergence, influence the intensification or decay of developed fronts. Of particular interest would be an examination of the energetics of the mature stages of baroclinic wave development, including the occluding process, as this is something that is suspected of being treated inaccurately by conventional numerical formulations. Note that the periodic semigeostrophic formulation might be applied to investigating baroclinic waves developing on an existing sharp front. Such an approach would be a significant departure from the usual way of investigating baroclinic waves numerically, which, following the pioneering work of Charney (1947) and Eady (1949) has typically been concerned only with modes evolving on a smooth baroclinic current rather than on a sloping thermal discontinuity. However, the former approach is much closer in spirit to the classical conceptual models of the Bergen school (Bjerknes, 1919; Bjerknes and Solberg, 1922). Finally, it would be illuminating to determine the extent to which a random, but smooth, initial state is able to convert its available potential energy to small-scale kinetic energy, and to what degree the increasing stratification is associated with the formation of surface fronts. It is speculated that the potentially coldest parcels of fluid will tend to spread out over an ever increasing proportion of the ground area, undercutting neighbouring warmer fluid by creating a succession of shallow fronts. Note that the constraint of potential enstrophy conservation, which limits the cascade of energy to small scales in two-dimensional or quasi-geostrophic turbulence, does not apply near the lower boundary of a semi-geostrophic model as potential vorticity (and hence enstrophy) is freely created or destroyed by frontal adjustments.

References

Bjerknes, J., 1919: On the structure of moving cyclones. Geofys.Publ., 1, No. 1, 1-8.

Bjerknes, J. and H. Solberg, 1922: Life cycle of cyclones and the polar front theory of atmospheric circulation. Geofys. Publ., 3, No. 1, 1-18.

Charney, J.G., 1947: The dynamics of long waves in a baroclinic westerly current, J. Met., 4, 135-163.

Cullen, M.J.P., 1983: Solutions to a model of a front forced by deformation. Quart. J. Roy. Meteor. Soc., 109, 565-573.

Cullen, M.J.P. and R.J. Purser, 1984: An extended Lagrangian theory of semi-geostrophic frontogenesis. J. Atmos. Sci., 41, 1441-1497.

Eady, E.T., 1949: Long waves and cyclone waves, Tellus, 1, 33-52.

Gill, A.E., 1981: Homogeneous intrusions in a rotating stratified fluid. J. Fluid Mech., 103, 275-293.

Hoskins, B.J., 1975: The geostrophic momentum approximation and the semi-geostrophic equations. J. Atmos. Sci., 32, 233-242.

Hoskins, B.J. and F.P. Bretherton, 1972: Atmospheric frontogenesis models: mathematical formulation and solutions. J. Atmos. Sci., 29, 11-37.

Hoskins, B.J. and I. Draghici, 1977: The forcing of ageostrophic motion according to the semi-geostrophic equations and in an isentropic coordinate model. J. Atmos. Sci., 34, 1859-1867.

Hoskins, B.J. and N. West, 1979: Baroclinic waves and frontogenesis II. Uniform potential vorticity jet flows - cold and warm fronts. J. Atmos. Sci., 36.

Purser, R.J. and M.J.P. Cullen, 1987: A duality principle in semi-geostrophic theory. J. Atmos. Sci., 44 (to appear).

Schubert, W.H., 1985: Semigeostrophic theory. J. Atmos. Sci., 42, 1770-1772.

Shutts, G.J., 1987: Balanced flow states resulting from penetrative slantwise convection. J. Atmos. Sci., 44 (to appear).

FIGURE CAPTIONS

Figure 1. Schematic cross-section through a finite-element solution showing the relationships among So, $\hat{So}$, $\underset{\sim}{b}$.

Figure 2. Illustrations to show the effect of 'padding' the margins of the support of ρ. (a) shows the solution with fronts corresponding to unpadded data (b). (c) shows the solution, with fronts smoothed out slightly, corresponding to the data. (d) modified by padding the shaded regions with small values of ρ.

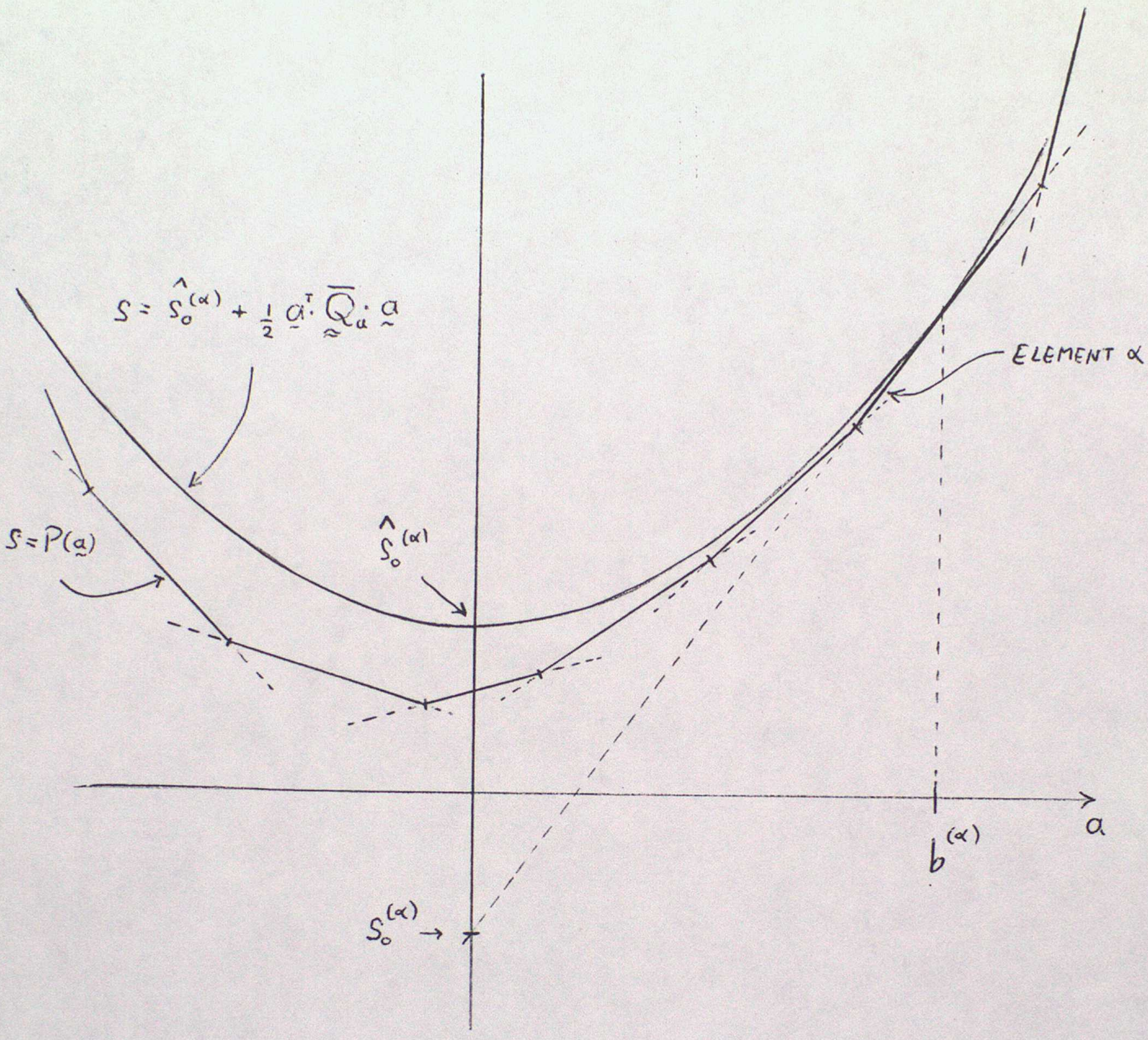
$s = \hat{s}_o^{(\alpha)} + \frac{1}{2}\,\underset{\sim}{a}^T \cdot \underset{\approx}{\overline{Q}}_\alpha \cdot \underset{\sim}{a}$
$s = P(\underset{\sim}{a})$
$\hat{s}_o^{(\alpha)}$
ELEMENT α
a
$b^{(\alpha)}$
$s_o^{(\alpha)}$

Figure 1

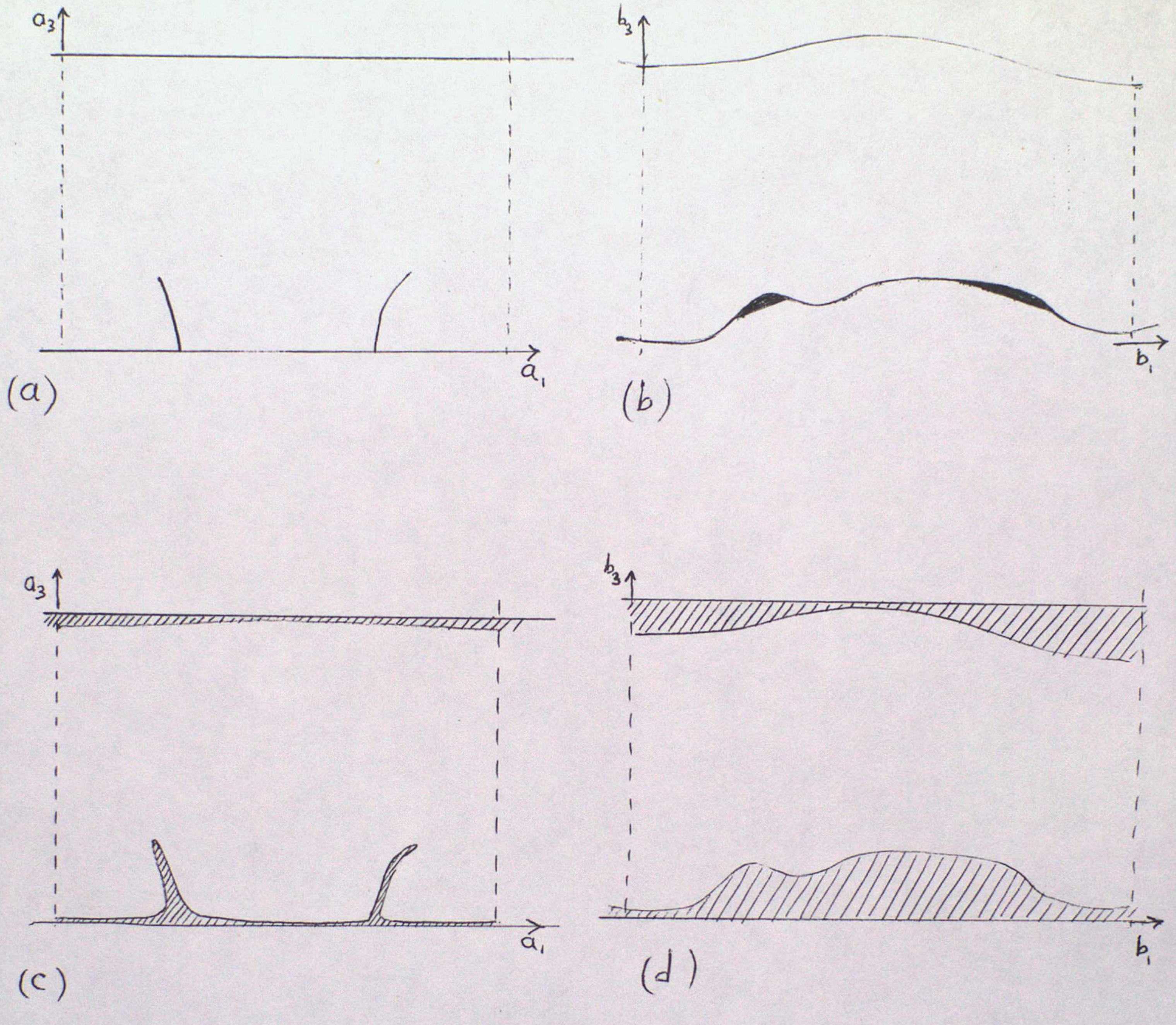

FIGURE 2